AAS 20-696

INITIAL RELATIVE-ORBIT DETERMINATION OF SPACE OBJECTS VIA RADIO FREQUENCY SIGNAL LOCALIZATION

Troy A. Henderson[*], Yasmeen Hack[†], Sophia Sunkin[‡], T. Alan Lovell[§], Joshuah Hess[¶], and Jessica Wightman[‖]

This paper presents a solution method for the initial orbit determination of a space-based transmitter using radio frequency measurements obtained from space-based receivers. Initial orbit determination requires a minimum of six independent measurements over time. Many radio frequency-based measurement equations can be expressed in polynomial form. The orbital motion of the transmitter is linearized relative to a reference orbit, which allows each radio frequency measurement to be expressed as a polynomial equation for the relative position and velocity of the transmitter at a chosen epoch time. The system of polynomials is then solved using known applied mathematics techniques.

INTRODUCTION

This research focuses on localization of a space object transmitting a radio frequency (RF) signal, as received by space-based platforms. RF localization of terrestrial objects has been widely studied[1,2,3,4,5] , and is often termed "geolocation." By contrast, RF localization of a space object, which is in effect an orbit determination problem, has received much less focus. The latter process will here be termed "astrolocation." In particular, this study examines the scenario of two cooperative receivers performing initial orbit determination (IOD) of a transmitter in close proximity. As such, an astrolocation technique can be based on the relative motion among the objects involved. Thus, the technique developed here will be termed initial relative orbit determination (IROD). This process is fundamentally represented in Figure 1 below.

Unlike the Global Positioning System (GPS) which uses a highly structured and well defined signal, the goal here is to be able to collect measurements that require no *a priori* information about the signal. One approach is to use time-difference-of-arrival (TDOA). Since the minimum number of platforms from which to extract TDOA is two, the scenarios explored will involve two orbiting receivers from which TDOA measurements are obtained.

[*]Associate Professor, Aerospace Engineering, Embry-Riddle Aeronauical University, 1 Aerospace Blvd., Daytona Beach, FL 32174.
[†]Undergraduate Student, Department of Mathematics, Colorado State University, Fort Collins, CO.
[‡]Student, Mission Viejo High School, Mission Viejo, CA.
[§]Senior Aerospace Engineer, Air Force Research Laboratory, Kirtland AFB, NM.
[¶]Assistant Professor, Aerospace Engineering, Air Force Institute of Technology, Dayton, OH.
[‖]Graduate Student, Aerospace Engineering, Air Force Institute of Technology, Dayton, OH.

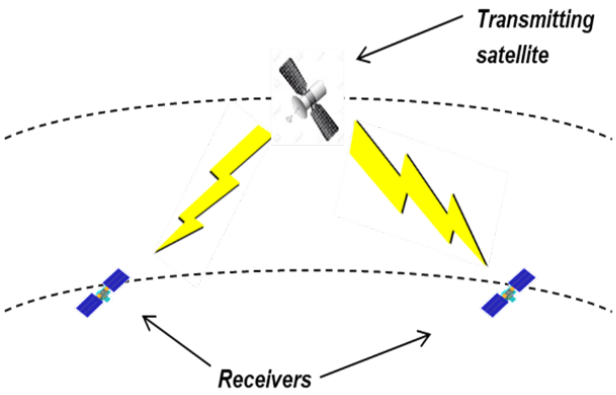

Figure 1. Graphical depiction of astrolocation.

TIME DIFFERENCE OF ARRIVAL AS MEASUREMENTS

The TDOA measurement is formed by comparing the transmitted signal received by two non-collocated receivers. By knowing the speed of the signal's propagation (in this case, the speed of light), the TDOA measurement can be related to the difference in the ranges from the transmitter's instantaneous location to that of the two receivers (i.e., the range difference of arrival or RDOA)

$$\begin{aligned}\Delta\rho_k &= c\Delta t_k = \rho_{2,k} - \rho_{1,k} \\ &= \left[(x_T - x_{r2,k})^2 + (y_T - y_{r2,k})^2 + (z_T - z_{r2,k})^2\right]^{\frac{1}{2}} \\ &- \left[(x_T - x_{r1,k})^2 + (y_T - y_{r1,k})^2 + (z_T - z_{r1,k})^2\right]^{\frac{1}{2}}\end{aligned} \tag{1}$$

where c is the speed of light, Δt_k is the instantaneous TDOA, $\rho_{1,k}$ is the range from the transmitter to Receiver 1, $\rho_{2,k}$ is the range from the transmitter to Receiver 2, (x_T, y_T, z_T) are the transmitter's instantaneous position coordinates, and (x_{r1}, y_{r1}, z_{r1}) and (x_{r2}, y_{r2}, z_{r2}) are the first and second receiver's instantaneous position coordinates.

Sinclair[5] then algebraically manipulated Equation 1 (including two instances of squaring both sides of the equation), resulting in a 2nd-order polynomial in terms of the transmitter's

instantaneous location, x_T, y_T, and z_T,

$$
\begin{aligned}
& x_T^2\left(\left(x_{r1,k}-x_{r2,k}\right)^2-\Delta\rho_k^2\right) \\
& +2x_Ty_T\left(x_{r1,k}-x_{r2,k}\right)\left(y_{r1,k}-y_{r2,k}\right) \\
& +2x_Tz_T\left(x_{r1,k}-x_{r2,k}\right)\left(z_{r1,k}-z_{r2,k}\right) \\
& +y_T^2\left(\left(y_{r1,k}-y_{r2,k}\right)^2-\Delta\rho_k^2\right) \\
& +2y_Tz_T\left(y_{r1,k}-y_{r2,k}\right)\left(z_{r1,k}-z_{r2,k}\right) \\
& +z_T^2\left(\left(z_{r1,k}-z_{r2,k}\right)^2-\Delta\rho_k^2\right) \\
& +x_T\left(\left(x_{r1,k}-x_{r2,k}\right)\left(K_{2,k}-K_{1,k}-\Delta\rho_k^2\right)+2\Delta\rho_k^2x_{r1,k}\right) \\
& +y_T\left(\left(y_{r1,k}-y_{r2,k}\right)\left(K_{2,k}-K_{1,k}-\Delta\rho_k^2\right)+2\Delta\rho_k^2y_{r1,k}\right) \\
& +z_T\left(\left(z_{r1,k}-z_{r2,k}\right)\left(K_{2,k}-K_{1,k}-\Delta\rho_k^2\right)+2\Delta\rho_k^2z_{r1,k}\right) \\
& +\frac{1}{4}\left(K_{2,k}-K_{1,k}-\Delta\rho_k^2\right)-\Delta\rho_k^2K_{1,k}=0
\end{aligned}
\tag{2}
$$

where $K_{i,k}=x_{i,k}^2+y_{i,k}^2+z_{i,k}^2$ is the square of the distance from the i^{th} receiver to the reference point at time t_k.

Geometrically, Equation 1 represents one sheet of a two-sheeted hyperboloid with the two receivers located at the foci. If four receivers were employed to obtain three simultaneous TDOA measurements, three coupled polynomials of the form of Equation 2 could be solved, yielding multiple solutions for x_T, y_T, and z_T. In an ideal (errorless) scenario, one of these solutions would be the transmitter's instantaneous location. Figure 2 depicts a geometric representation of this process, whereby three single-sheeted hyperboloids are intersected to locate the transmitter.

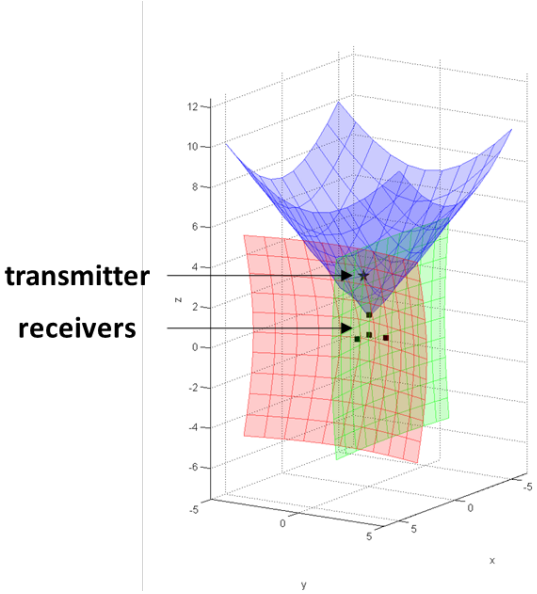

Figure 2. Geometric depiction of TDOA localization.

RELATIVE MOTION DYNAMICS

Whereas TDOA is demonstrated above as a technique for instantaneous localization, astrolocation scenarios entail two primary differences from static (e.g. terrestrial) scenarios. First, the fact that the transmitter is in orbit means there are six parameters governing its state, thus six TDOA measurements are required. Second, because the six TDOAs do not all have to be obtained simultaneously but rather over time, astrolocation can be achieved with only two receivers. Shuster[6] first extended the above development for astrolocation. By incorporating a model of the transmitter's orbital motion, each TDOA measurement can be mapped back to an epoch time, in the fashion of classical orbit determination. For this paper, the relative motion of the transmitter with respect to a defined reference orbit will be incorporated via the well known Clohessy-Wiltshire (CW) solution.[7]

When considering spacecraft that are moving in the vicinity of each other, such that $\rho/R << 1$, we can approximate the motion by linearizing the relative equations of motion. Schaub and Junkins,[8] among numerous others, derive the equations of unforced relative motion for circular chief orbits, the Clohessy-Wiltshire equations,[7] as

$$\ddot{x} - 2n\dot{y} = 0 \tag{3a}$$

$$\ddot{y} + 2n\dot{x} - 3n^2 y = 0 \tag{3b}$$

$$\ddot{z} + n^2 z = 0 \tag{3c}$$

where $n = \sqrt{\mu/a^3}$ is the mean motion of the reference orbit. The CW dynamics equations have the following analytical solution:

$$x(t) = x_0\left(4 - 3\cos nt\right) + \frac{\dot{x}_0}{n}\sin nt + \frac{2\dot{y}_0}{n}\left(1 - \cos nt\right) \tag{4a}$$

$$y(t) = 6x_0\left(\sin nt - nt\right) + y_0 + \frac{2\dot{x}_0}{n}\left(\cos nt - 1\right) + \frac{\dot{y}_0}{n}\left(4\sin nt - 3nt\right) \tag{4b}$$

$$z(t) = z_0\cos nt + \frac{\dot{z}_0}{n}\sin nt \tag{4c}$$

By re-writing the solution to the dynamics, we can obtain the state transition matrix and identify appropriate sub-matrix blocks,

$$\left[\begin{array}{c|c} \phi_{rr} & \phi_{rv} \\ \hline \phi_{vr} & \phi_{vv} \end{array}\right] = \left[\begin{array}{ccc|ccc} 4-3\cos nt & 0 & 0 & \frac{1}{n}\sin nt & \frac{2}{n}\left(1-\cos nt\right) & 0 \\ 6\left(\sin nt - nt\right) & 1 & 0 & \frac{2}{n}\left(\cos nt - 1\right) & \frac{1}{n}\left(4\sin nt - 3nt\right) & 0 \\ 0 & 0 & \cos nt & 0 & 0 & \frac{1}{n}\sin nt \\ \hline 3nt\sin nt & 0 & 0 & \cos nt & 2\sin nt & 0 \\ 6n\left(\cos nt - 1\right) & 0 & 0 & -2\sin nt & 4\cos nt - 3 & 0 \\ 0 & 0 & -n\sin nt & 0 & 0 & \cos nt \end{array}\right] \tag{5}$$

such that

$$\begin{pmatrix} x(t) \\ y(t) \\ z(t) \\ \dot{x}(t) \\ \dot{y}(t) \\ \dot{z}(t) \end{pmatrix} = \begin{bmatrix} \phi_{rr} & \phi_{rv} \\ \phi_{vr} & \phi_{vv} \end{bmatrix} \begin{pmatrix} x(t_0) \\ y(t_0) \\ z(t_0) \\ \dot{x}(t_0) \\ \dot{y}(t_0) \\ \dot{z}(t_0) \end{pmatrix} \tag{6}$$

As the measurement polynomial in Eqn (2) only involves the transmitter's instantaneous position, we are only interested in the ϕ_{rr} and ϕ_{rv} portions of the state transition matrix. Therefore, we can write

$$x_{i,k} = (4 - 3\cos nt_k) \cdot x_{i,0} + \frac{1}{n}\sin nt_k \cdot \dot{x}_{i,0} + \frac{2}{n}(1 - \cos nt_k) \cdot \dot{y}_{i,0} \tag{7a}$$

$$y_{i,k} = 6(\sin nt_k - nt_k) \cdot x_{i,0} + y_{i,0} + \frac{2}{n}(\cos nt_k - 1) \cdot \dot{x}_{i,0} + \frac{1}{n}(4\sin nt_k - 3nt_k) \cdot \dot{y}_{i,0} \tag{7b}$$

$$z_{i,k} = \cos nt_k \cdot z_{i,0} + \frac{1}{n}\sin nt_k \cdot \dot{z}_{i,0} \tag{7c}$$

Alternatively,

$$x_{i,k} = \phi_{rr_1}\vec{r}_i(t_0) + \phi_{rv_1}\dot{\vec{r}}_i(t_0) \tag{8}$$

$$y_{i,k} = \phi_{rr_2}\vec{r}_i(t_0) + \phi_{rv_2}\dot{\vec{r}}_i(t_0) \tag{9}$$

$$z_{i,k} = \phi_{rr_3}\vec{r}_i(t_0) + \phi_{rv_3}\dot{\vec{r}}_i(t_0) \tag{10}$$

where ϕ_{rr_i} and ϕ_{rv_i} indicate the i^{th} row of ϕ_{rr} and ϕ_{rr}, respectively. Inserting these expressions for x_T, y_T, and z_T into Equation 2 yields a second-order polynomial of the form

$$a_1 x_T^2(t_0) + a_2 x_T(t_0) y_T(t_0) + a_3 x_T(t_0) z_T(t_0) + a_4 x_T(t_0) \dot{x}_T(t_0) + \cdots + a_{28} = 0 \tag{11}$$

where the unknowns are the transmitter's initial relative conditions. If we obtain N RDOA measurements at unique times, we can determine these initial conditions by solving the system of coupled polynomials. For a square system, N should be the number of variables.

Consider a scenario involving the transmitter orbit and the two receiver orbits coplanar with the reference orbit such that all spacecraft have $z(t) = \dot{z}(t) = 0$. In such cases, the transmitter's motion is planar (2D) and governed by only four variables: x, y, $\dot{x}$, and $\dot{y}$. Here the polynomials remain second-order, but each with 15 total terms instead of 28. Also, $N = 4$, therefore only four RDOA measurements are needed.

POLYNOMIAL SCALING

The TDOA IROD system of equations have been found to result in a system of poorly conditioned polynomials.[5] Each of the coefficients of these polynomial systems vary by several orders of magnitude, resulting in an incredibly high amount of precision required to solve the polynomial system with an acceptable level of accuracy. According to Morgan[9]

, "The purpose of scaling is to reduce the possibility of catastrophic arithmetic problems when a solution method is evoked on a computer." Similar to Morgan's SCLGEN algorithm, we employ a two-step scaling process which applies scaling to both the individual variables and the equation as a whole. Variable scaling makes use of a change of variable of the form $\bar{x} = 10^{c_1}x$, and similar for the other variables. Equation scaling reduces the order of the polynomial coefficients across the entire equation in the form $\bar{f}_1 = 10^{c_5}f_1 = 0$, where all c_i are non-zero values. Therefore, in the planar scenarios, we have eight scaling constants–four for the variables and four for the equations. In the 3D case, we have twelve scaling constants–six for the variables and six for the equations (note the planar case scaling is described above).

Referring to Equation 11, the system of polynomials can be rewritten as

$$10^{c_N}\left[10^{2c_1}a_1\bar{x}_T^2 + 10^{c_1}10^{c_2}a_2\bar{x}_T\bar{y}_t + ...a_{28}\right] = 0 \tag{12}$$

We seek to make the conditioning of the polynomials improved, meaning centering the coefficients around unity while simultaneously minimizing the variance of the coefficients. After collecting terms around the polynomial components and labeling them as E, we sum square the exponents

$$r_{1,1} = \sum_{i=1}^{N} E_{1,i}^2 \tag{13}$$

$$r_{1,2} = \sum_{i=1}^{N}\sum_{j>i}^{N}\left(E_{1,i} - E_{1,j}\right)^2 \tag{14}$$

$$r_1 = r_{1,1} + r_{1,2} \tag{15}$$

The the total cost function r is given by the sum of quadratics, $r = r_1 + r_2 + \cdots + r_N$, which sums over all equations and all variables. Since the cost function is a sum of squares of the scaling variables and constant terms, the global minimum can be found analytically by

$$\frac{dr}{dc_i} = 0 \tag{16}$$

which has the form $[A]\vec{c} = \vec{b}$, where $[A]$ is a constant matrix, $\vec{c}$ is the vector of scaling coefficients, and $\vec{b}$ is a vector which is a function of the original coefficients.

The result is a system of equations that is much easier solved using a numerical method with a limited amount of machine precision.

SCENARIO DEFINITIONS

The current work focuses on three planar (2D) scenarios, as they demonstrate the algorithms necessary for solution. The initial relative orbit conditions chosen for each spacecraft are given in Table 1. Note that the two receiver orbits maintain the same initial conditions across both scenarios, and only the transmitter's initial conditions differ. The initial conditions are given that define the three scenarios.

Table 1. Scenario definitions

	Transmitter(1)	Transmitter(2)	Transmitter(3)	Receiver 1	Receiver 2
$x(t_0), km$	1	4.5	8.22	10	8
$y(t_0), km$	11	7	9.16	-5	3
$\dot{x}(t_0), km/s$	0.012	-0.022	0.038	0.001	0.01
$\dot{y}(t_0), km/s$	0.03	0.05	-0.044	-0.02263	-0.008102

The relevant scenario data was generated by assuming a circular reference orbit about Earth of radius 6778 km. Measurement times were taken at intervals of one-tenth of an orbit period of the reference orbit, or

$$(t_0, t_1, t_2, t_3) = (0,\ 555.3,\ 1110.7,\ 1666.0) \text{ seconds}$$

The translational states of each of the three spacecraft were then computed at each measurement time using the CW equations of motion. Next, the RDOA in Equation 1 and polynomial coefficients of Equation 2 were computed at each time step.

For the purpose of solution disambiguation (discussed below), a fifth measurement time was added, one-tenth of an orbit period after the final measurement, or $t_5 = 2276.7$ seconds.

SOLUTION METHODS

For this work, two polynomial root-solving methods were used. Macaulay's method[10,11] is based on resultants. As Macaulay's resultants are expressed in terms of determinants, they can be used to translate root-finding problems into eigenvalue problems. Bertini[12] is a software package that numerically solves systems of polynomial equations using homotopy continuation. For this work, Macaulay was implemented in MATLAB and Bertini was downloaded from the website.[13]

Polynomial scaling was used with both polynomial root-solving methods, resulting in four solution methods as described in Table 2.

Table 2. Solution methods definitions

Name	Root-Solver	Scaling
Method 1	Macaulay	N
Method 2	Macaulay	Y
Method 3	Bertini	N
Method 4	Bertini	Y

According to Bézout's Theorem,[14] the number of finite solutions to a square system is a^b where a is the highest degree of the polynomials and b is the number of variables. For the planar case, this results in $2^4 = 16$ finite solutions, and for the 3D case, $2^6 = 64$ finite solutions. As such, for this work we expect 16 finite solutions to be produced by each method, and this will be used as a metric on the solution methods.

RESULTS

This section presents a comparison of results for the scenarios. For each scenario, the polynomials were solved utilizing the four solution methods as described in Table 2. Finally, a method is presented which clearly identifies the correct solution by disambiguation of the solutions.

Scenario 1

Recall that Table 1 displays the true values used to simulate Scenario 1. The analysis of Scenario 1 follows.

Figure 3 shows the root mean square (RMS) value of the polynomial residual yielded by each (x_T, y_T, z_T) solution found by each method. This RMS metric is given by

$$x_{RMS} = \sqrt{(x_1^2 + x_2^2 + x_3^2 + x_4^2)/4} \tag{17}$$

where x_1 is the right hand side of the polynomial of the form of Equation 11 at the first measurement time when the solution values of x_0, y_0, $\dot{x}_0$, and $\dot{y}_0$ are inserted; x_2 is the right hand side of the polynomial at the second measurement time; and so forth.

Ideally, the RMS residual value for each solution is zero, so Fig. 3 provides a metric of how well each solution method was able to solve the polynomial system. It is obvious that the Method 1 (Macaulay applied to the original polynomial system) did not perform accurately. Additionally, Method 1 returned 18 solutions, instead of the expected 16 solutions, to the original polynomial system. However, Methods 2-4 each yield 16 solutions, with much lower residuals (on the order of 10^{-2} km^4 or below), signifying these methods solved the system well.

As a point of comparison, the order of magnitude ratio between the largest and smallest (non-zero) coefficients in the original, unscaled system was 10^9 and the condition number of the polynomial coefficients was 6.095×10^5. For the scaled system, the order of magnitude ratio between the largest and smallest coefficients was 10^4 and the condition number was reduced to 5.2997×10^2.

Figure 4 shows the root mean square (RMS) value of the RDOA residual yielded by each solution. At each measurement time, the RDOA residual is computed by inserting the x_T, y_T, and z_T solution into Equation 1 to obtain the calculated RDOA, then subtracting from the actual RDOA. As this was a simulated scenario, the actual RDOA was computed and known, but in a practical mission scenario, the RDOA would be measured via signal processing (i.e. known with some uncertainty).

Because the algebraic manipulation from Equation 1 to Equation 2 involves two instances of squaring both sides of an equation, it is expected that not all 16 solutions to the polynomials will satisfy the original RDOA equations. The purpose of computing the RDOA residual then is to disambiguate these extraneous solutions. The figure indicates that the Method 1 solutions yield RDOA residuals ranging from order 10^{-3} to order 10^2. Methods 2-4 each yield two solutions with RDOA residual values of order 10^{-7} or less,

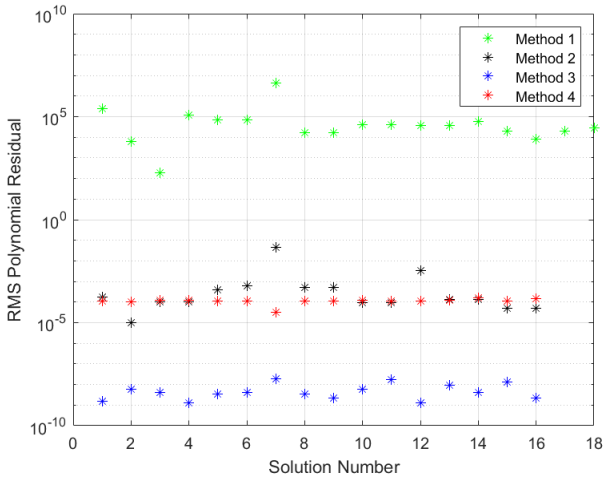

Figure 3. Polynomial residual for Scenario 1 (units are km^4).

and 14 solutions with RDOA residual values of order 10^1 or 10^2. Table 3 shows the two lowest RDOA residual solutions for Methods 2-4. (Note that Method 1 is ignored from the table due to the high RDOA error.) From these results, we conclude that there exist two solutions to the original RDOA equations for this scenario, one of which is of course the actual transmitter relative orbit.

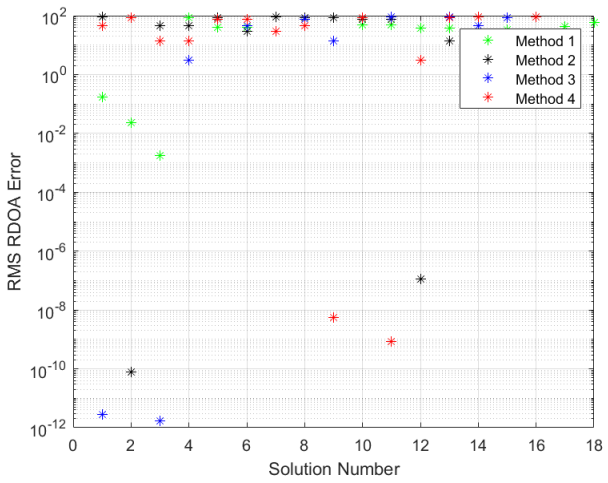

Figure 4. RDOA residual for Scenario 1 (units are km).

Comparing the values in Table 3 with the actual transmitter initial conditions in Table 1, we see that Methods 2-4 each yield the actual transmitter initial conditions to at least four decimal place accuracy. The other solution in the table can be disambiguated by simulating an extra (fifth) RDOA measurement, which only the true solution can be shown to satisfy. Figure 5 shows the RDOA error for Methods 1 and 2. Notice that for the scaled polynomial solution (Method 2), index 2 has a similar RDOA error, whereas solution index 7 has a

Table 3. Scenario 1 Results

Value	Method 3	Method 4	Method 2
$x(t_0)_1, km$	0.9999+2.2039e-15i	1.0000+1.8415e-16i	1.0000
$y(t_0)_1, km$	11.0000-3.1296e-15i	11.0000+2.9633e-16i	11.0000
$\dot{x}(t_0)_1, km/s$	0.0120-1.4352e-18i	0.0120+3.1000e-19i	0.0120
$\dot{y}(t_0)_1, km/s$	0.0300-1.2766e-17i	0.0300+3.0262e-19i	0.0300
$x(t_0)_2, km$	4.4420+4.1027e-19i	4.4420-5.7957e-14i	4.4420
$y(t_0)_2, km$	6.2422-1.0081e-18i	6.2422+7.7120e-14i	6.2422
$\dot{x}(t_0)_2, km/s$	0.0247-2.3899e-21i	0.0247+2.4027e-16i	0.0247
$\dot{y}(t_0)_2, km/s$	-0.0009-1.1907e-21i	-0.0009+1.5554e-16i	-0.0009

large change in RDOA error with the addition of the 5^{th} measurement. Bertini results (from Methods 3 and 4) demonstrate similar disambiguation properties. Therefore, we are confident that the true solution to the transmitter initial relative state was found.

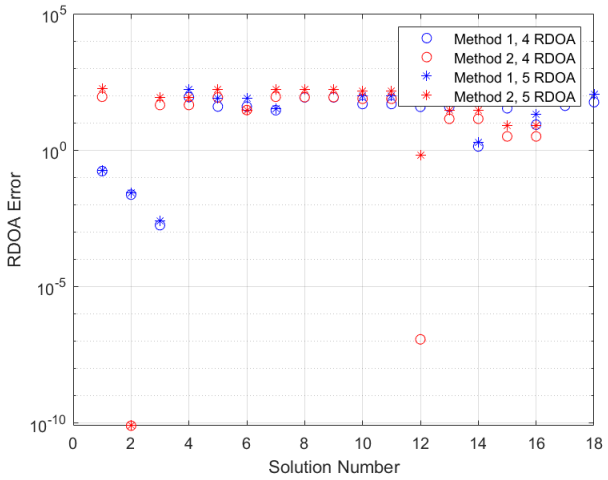

Figure 5. RDOA residual with 5^{th} measurement for Scenario 1 (units are km).

Scenario 2

Recall that Table 1 displays the true values used to simulate Scenario 2. The analysis follows.

Figure 6 shows the root mean square (RMS) values of the polynomial residual. Again, Method 1 did not perform accurately, returning only 13 solutions, all of them yielding high polynomial residuals. Method 2 returned 22 solutions with wide variation in residual values: 6 of them were above 10^{11}, two were of order 10^3, and the remaining 14 were order 10^{-2} or below. Method 3 returned 16 solutions with all residual values of order 10^{-6} or below, and Method 4 also returned 16 solutions with all residual values of order 10^{-2} or below.

As a point of comparison, the order of magnitude ratio between the largest and smallest

(non-zero) coefficients in the original, unscaled system was 10^9 and the condition number of the polynomial coefficients was 1.6772×10^6. For the scaled system, the order of magnitude ratio between the largest and smallest coefficients was 10^4 and the condition number was reduced to 1.0163×10^3.

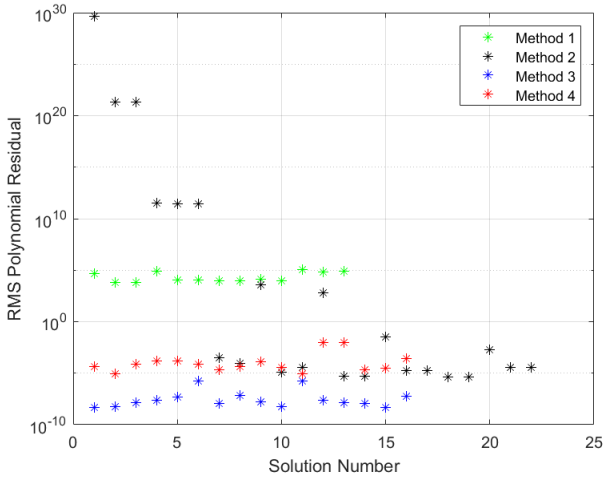

Figure 6. Polynomial residual for Scenario 2 (units are km^4).

Figure 7 shows the root mean square (RMS) value of the RDOA residuals. The Method 1 solutions yield RDOA residuals ranging from order 10^{-2} to order 10^2. Methods 2-4 each yield two solutions with RDOA residual values of order 10^{-9} or less, with the remaining residual values of order 10^2. Table 4 shows the two lowest RDOA residual solutions for Methods 2-4. Again we conclude that there exist two solutions to the original RDOA equations for this scenario, and again we see that Methods 2-4 each yield the actual transmitter initial conditions to several decimal place accuracy.

Table 4. Scenario 2 Results

Value	Method 3	Method 4	Method 2
$x(t_0)_1, km$	4.5000-1.3446e-15i	4.5000+2.3592e-15i	4.5000
$y(t_0)_1, km$	7.0000+3.8100e-15i	7.0000-3.0616e-15i	7.0000
$\dot{x}(t_0)_1, km/s$	-0.02200-1.7369e-18i	-0.0220+2.2918e-18i	-0.0220
$\dot{y}(t_0)_1, km/s$	0.0500+1.0680e-17i	0.0500-7.4323e-18i	0.0500
$x(t_0)_2, km$	-7.3008-6.3417e-17i	-7.3008-2.0800-14i	-7.3008
$y(t_0)_2, km$	26.2213+1.0809e-16i	26.2213+3.5745e-14i	26.2213
$\dot{x}(t_0)_2, km/s$	0.08202+3.0028e-19i	0.08211+9.4893e-17i	0.0820
$\dot{y}(t_0)_2, km/s$	0.003815+7.0990e-20i	0.003815+2.4885e-17i	0.0038

The other solution in the table can be disambiguated by simulating an extra (fifth) RDOA measurement, which only the true solution can be shown to satisfy. Figure 8 shows the RDOA error for Methods 1 and 2. Notice that for the scaled polynomial solution (Method 2), index 9 has a similar RDOA error, whereas solution index 17 has a large change in RDOA error with the addition of the 5^{th} measurement. Bertini results (from Methods 3 and

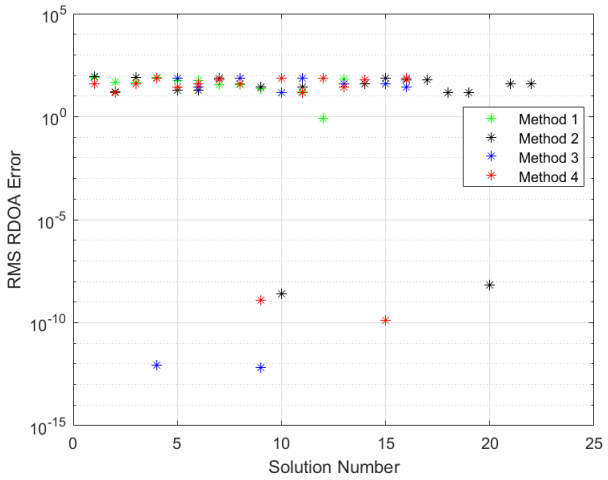

Figure 7. RDOA residual for Scenario 2 (units are km).

4) demonstrate similar disambiguation properties. Therefore, we are confident that the true solution to the transmitter initial relative state was found.

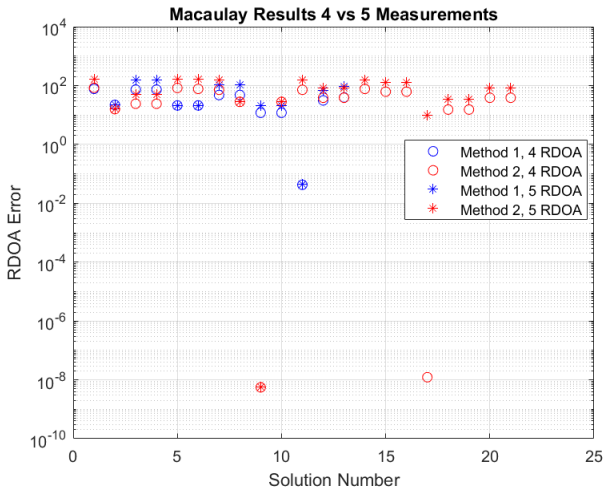

Figure 8. RDOA residual with 5^{th} measurement for Scenario 2 (units are km).

Scenario 3

Recall that Table 1 displays the true values used to simulate Scenario 3. The analysis follows.

Figure 9 shows the root mean square (RMS) values of the polynomial residual. Again, Method 1 did not perform accurately, returning only 14 solutions, all of them yielding relatively high polynomial residuals. Methods 2 through 4 returned 16 solutions each, all with RMS polynomial residuals under 10^{-1}. Note that Method 2, Macaulay applied to the

scaled polynomial system, solved the equations most accurately. Methods 3-4, both using Bertini did not show significant improvement in solution accuracy when using the scaled equations.

As a point of comparison, the order of magnitude ratio between the largest and smallest (non-zero) coefficients in the original, unscaled system was 10^{10} and the condition number of the polynomial coefficients was 3.7057×10^6. For the scaled system, the order of magnitude ratio between the largest and smallest coefficients was 10^4 and the condition number was reduced to 5.7144×10^2.

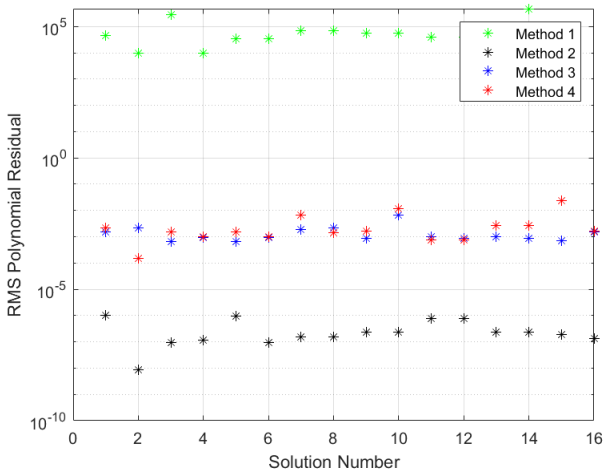

Figure 9. Polynomial residual for Scenario 3 (units are km^4).

Figure 10 shows the RMS value of the RDOA residuals. The Method 1 solutions yielded RDOA residuals ranging from order 1 to order 10^2. Methods 2-4 each yield two solutions with RDOA residual values of order 10^{-7} or less, with the remaining residual values of order 10^1. Table 5 shows the two lowest RDOA residual solutions for Methods 2-4. Again we conclude that there exist two solutions to the original RDOA equations for this scenario, and again we see that Methods 2-4 each yield the actual transmitter initial conditions to several decimal place accuracy.

Table 5. Scenario 3 Results

Value	Method 3	Method 4	Method 2
$x(t_0)_1, km$	8.2200-1.1973e-14i	8.2200-2.5852e-15i	8.2200
$y(t_0)_1, km$	9.1600+1.5048e-14i	9.1600+3.2551e-14i	9.1600
$\dot{x}(t_0)_1, km/s$	0.0380 + 6.5515e-17i	0.0380+1.0621e-16i	0.0380
$\dot{y}(t_0)_1, km/s$	-0.0440-2.6219e-17i	-0.0440-8.3680e-17i	-0.0440
$x(t_0)_2, km$	-0.2625 - 1.3536e-14i	-0.2625 + 4.7576e-13i	-0.2625
$y(t_0)_2, km$	19.4337 + 2.9460e-14i	19.4337- 1.0286e-12i	19.4337
$\dot{x}(t_0)_2, km/s$	0.0766 + 1.2367e-16i	0.0767 - 3.4358e-15i	0.0766
$\dot{y}(t_0)_2, km/s$	-0.0548 - 7.7332e-17i	-0.0548 + 1.7873e-15i	-0.0548

The other solution in the table can be disambiguated by simulating an extra (fifth) RDOA

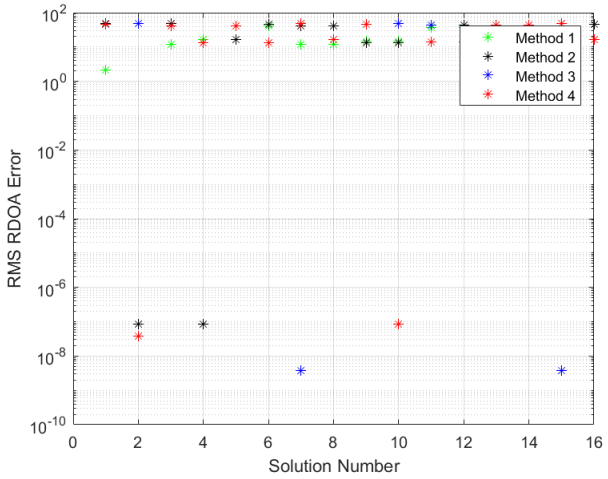

Figure 10. RDOA residual for Scenario 3 (units are km).

measurement, which only the true solution can be shown to satisfy. Figure 11 shows the RDOA error for Methods 2-4. Notice that for the scaled polynomial Macaulay solution (Method 2), index 4 has a similar RDOA error, whereas solution index 2 has a large change in RDOA error with the addition of the 5^{th} measurement. Bertini results (from Methods 3 and 4) demonstrate similar disambiguation properties. Therefore, we are confident that the true solution to the transmitter initial relative state was found.

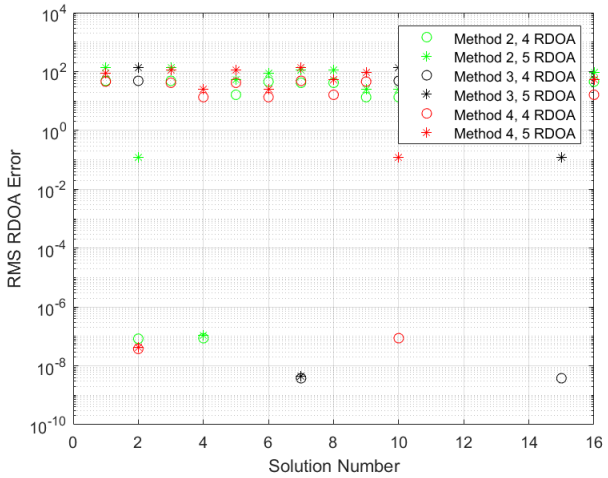

Figure 11. RDOA residual with 5^{th} measurement for Scenario 3 (units are km).

CONCLUSION

In conclusion, the problem of astrolocation via RF transmission has been defined, measurements converted to a polynomial system, and solutions provided using multiple methods. Bertini was shown to solve the system of polynomials well, while Macaulay struggled

to find a reasonable solution without the aid of polynomial scaling. When scaling was applied, Macaulay generally found answers that were correct to several decimal places. Bertini applied to the scaled problem also found accurate solutions. Bertini, in both unscaled and scaled cases, found the correct solution with extremely small imaginary components, likely due to machine precision.

Future work will investigate full 3D scenarios, computation time, statistical uncertainty models, and implementation on flight-like hardware.

REFERENCES

[1] Ho and Chan, "Solution and performance analysis of geolocation by TDOA," *IEEE Transactions on Aerospace and Electronic Systems*, Vol. 29, No. 4, 1993, pp. 1311–1322.

[2] Levanon, "Quick position determination using 1 or 2 LEO satellites," *IEEE Transactions on Aerospace and Electronic Systems*, Vol. 34, No. 3, 1998, pp. 736–754.

[3] Pattison and Chou, "Sensitivity analysis of dual satellite geolocation," *IEEE Transactions on Aerospace and Electronic Systems*, Vol. 36, No. 1, 2000, pp. 56–71.

[4] Mason and Romero, "TOA/FOA geolocation solutions using multivariate resultants," *Navigation*, Vol. 52, No. 3, 2005, pp. 163–177.

[5] Sinclair, Lovell, and Darling, "RF localization solution using heterogeneous TDOA," *Proceedings of IEEE Aerospace Conference*, March 2015.

[6] Shuster, Sinclair, and Lovell, "Initial Relative-Orbit Determination using Heterogeneous TDOA," *Proceedings of IEEE Aerospace Conference*, March 2017.

[7] Clohessy and Wiltshire, "Terminal guidance system for satellite rendezvous," *Journal of the Aerospace Sciences*, Vol. 27, No. 9, 1960, pp. 653–658.

[8] Schaub and Junkins, *Analytical Mechanics of Space Systems*. AIAA Education Series, 2003.

[9] Morgan, *Solving Polynomial Systems Using Continuation for Engineering and Scientific Problems*. Prentice-Hall, 1987.

[10] Macaulay, *The Algebraic Theory of Modular Systems*. Cambridge University Press, 1916.

[11] Macaulay, "On some formulae in elimation," *Proceedings of the Londong Mathematical Society*, Vol. 35, 1902, pp. 3–27.

[12] Bates, Hauenstein, Sommese, and Wampler, *Numerically solving polynomial sytems with Bertini*. SIAM, 2013.

[13] Bates, Hauenstein, Sommese, and Wampler, "Bertini Home Page," `https://bertini.nd.edu`, July 2020.

[14] Coolidge, *A Treatise on Algebraic Plane Curves*. Dover, 1959.